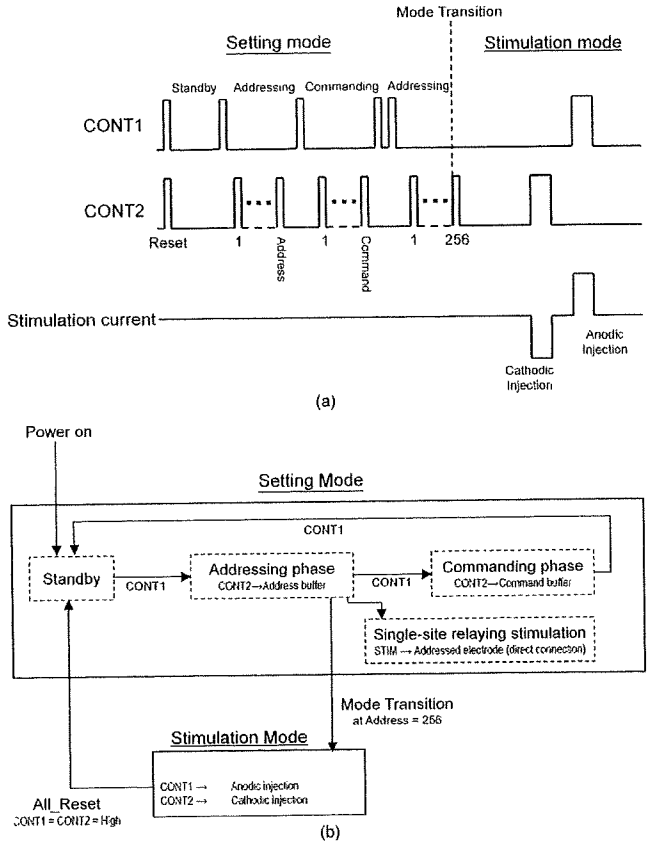

Fig. 2. Operation sequence for the unit chip.

As shown in Fig. 2, the unit chip has two operation modes. When the unit chip is reset, it is in the setting mode. Each unit chip accepts and stores a control command which defines the function to be used and the conditions for retinal stimulation. After we set the commands on the unit chips, we change the operation mode into a stimulation mode to perform retinal stimulation using the on-chip stimulator. The stimulation output is prohibited in the setting mode, except for single-site relaying stimulation which is described later.

In the setting mode, there are two listening phases: addressing and commanding. The listening phase is defined by a 3-b asynchronous ring scanner clocked by CONT1. At the beginning of the addressing phase, a 9-b asynchronous counter called the address buffer in the control logic is reset. All the unit chips then count the pulses applied to CONT2 and compare them to 8-b chip IDs that are unique to each unit chip. After the unit chip address is applied, the listening phase is changed into the commanding phase with a pulse on CONT1. In the commanding phase, the pulse applied on CONT2 is relayed to an 8-b counter called the command buffer only when the value in the address buffer is the same as the chip ID. The number of pulses for the CONT2 input is stored in the command buffer on the selected unit chip and interpreted as the specific operation condition provided for the unit chip. Table II shows the command table. The command includes the stimulation current for the on-chip stimulator and additional instructions. In contrast to the address buffer, the command buffer is not reset throughout the operation. After the pulses on CONT2, to define the operation conditions for the selected unit chip, we apply

TABLE II
COMMAND TABLE

Bit 1	Enable 50 μA
Bit 2	Enable 100 μA
Bit 3	Enable 200 μA
Bit 4	Enable 300 μA
Bit 5	Enable 400 μA
Bit 6	Enable light-controlled stimulation using on-chip stimulator
Bit 7	Enable light-controlled relaying stimulation using external stimulator
Bit 8	Enable unconditional relaying stimulation using external stimulator

*Default operation = unconditional stimulation using on-chip stimulator

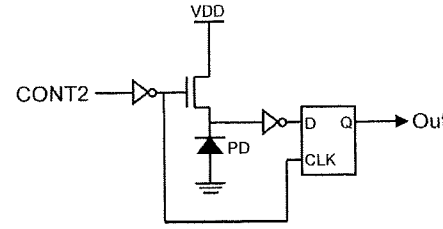

Fig. 3. Schematic for the light-controlled decision circuitry.

pulses on CONT1 to start another address and command for the next unit chip.

After we set the conditions for all the unit chips to be used for stimulation, we change the operation mode from the setting mode to the stimulation mode. To change the operation mode, the ninth bit of the address buffer is turned on H by applying 256 pulses on CONT2 in the addressing phase. Once the ninth bit becomes H, a 1-b flag resistor called a "stim flag" is put on H until the device is reset. Since the input of the command buffer is blocked in the stimulation mode, we can use CONT1 and CONT2 to trigger the stimulation. We use CONT1 and CONT2 to control the anodic and cathodic current injection. The stimulator was designed for symmetric injection, and the durations of the CONT1 and CONT2 pulses should be the same if we want to maintain charge balance during the stimulation.

Light-controlled stimulation is one of the most important functional extensions in the present design. We implemented a light-controlled decision for local stimulation, in which the stimulation is enabled when the local light intensity is higher than a threshold value. We implemented an active pixel sensor with binary output, shown in Fig. 3. The layout of the circuitry is shown in the inset in Fig. 1. The size of the photodiode was 5 μm × 5 μm. In contrast to conventional CMOS image sensor pixels, VDD was used as the reset voltage. Although this may cause nonlinearity in the sensitivity curve, we can implement the light-controlled functionality without any additional input. A comparator directly connected to the photodiode node transforms the photodiode level into a binary output. It is very important that the photodiode is reset and that the comparator is latched when CONT2 is low. The photodiode starts to discharge at the L-to-H transition for each pulse on CONT2, and the decision at the H-to-L transition of the pulse is latched until the next pulse is applied. This means that the

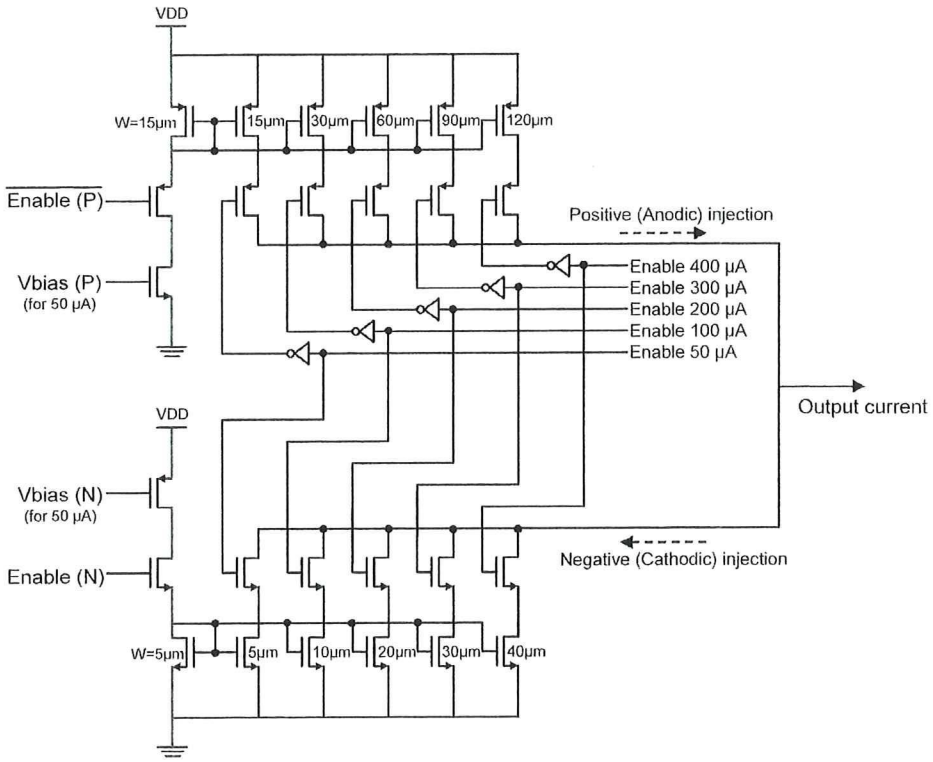

Fig. 4. Schematic for the bidirectional constant-current stimulator.

threshold light intensity for light-controlled decisions can be adjusted with the length of the last pulse in the commanding phase. We implemented both light-controlled and unconditional stimulation. When we perform the light-controlled decision for the stimulation, the length of the last pulse in the commanding phase is adjusted to provide the appropriate threshold.

The single-site relaying stimulation is implemented within the setting mode. Since the stimulation function is disabled in all the unit chips in the setting mode, we can realize single-site stimulation with no additional control to disable the other unit chips. The only control sequence for single-site relaying stimulation is to send the "direct connection" command to one of the unit chips. The "direct connection" function is activated when the seventh or eighth bit of the command buffer is set at H. The single-site relaying stimulation mode can be controlled by light as well.

We implemented a bidirectional current injector as the on-chip stimulator. Fig. 4 shows the schematic of the stimulator circuitry. The stimulator consists of a pair of NMOS and PMOS current sources. The gate widths of the MOS current regulators are designed to flow at 50, 100, 200, 300, and 400 μA. The injection current for the stimulation can be varied using combinations of these current regulators. The current regulator lines to be used are defined by the lower 5 b of the commend buffer (Enable 50 μA–Enable 400 μA). The injection switches of the selected current regulator lines in the PMOS current source are closed when CONT1 is H, and the injection switches in the NMOS current source are closed when CONT2 is H.

In the die design, we placed a set of unit chip cores with different chip IDs on one die. We used two kinds of connection structures. One is external pads around the unit chip core (pad type), and the other is preconnected wires which will be transformed into a flexible bus wiring (padless type). Using the external pads, the CMOS die is bonded onto a flexible

TABLE III
VARIATIONS OF THE RETINAL STIMULATOR CHIPS

Chip type	(a)	(b)	(c)
Layout	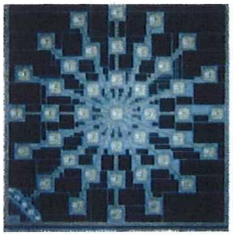 4000 μm	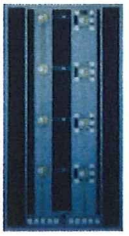 1500 μm	 600 μm
Electrodes per unit chip	1		9
Stimulation	Multi-site		Single-site
On-chip stimulator	Implemented		Not implemented
Number of unit chips on die	41	4 x 2 types	4
Connection type	Padless	Pad / Padless	Pad
Light sensing circuit	This work (Fig. 3)		
Lifetime in wet environment	Not yet		Over 10 days
In vivo demonstration	Not yet		This work

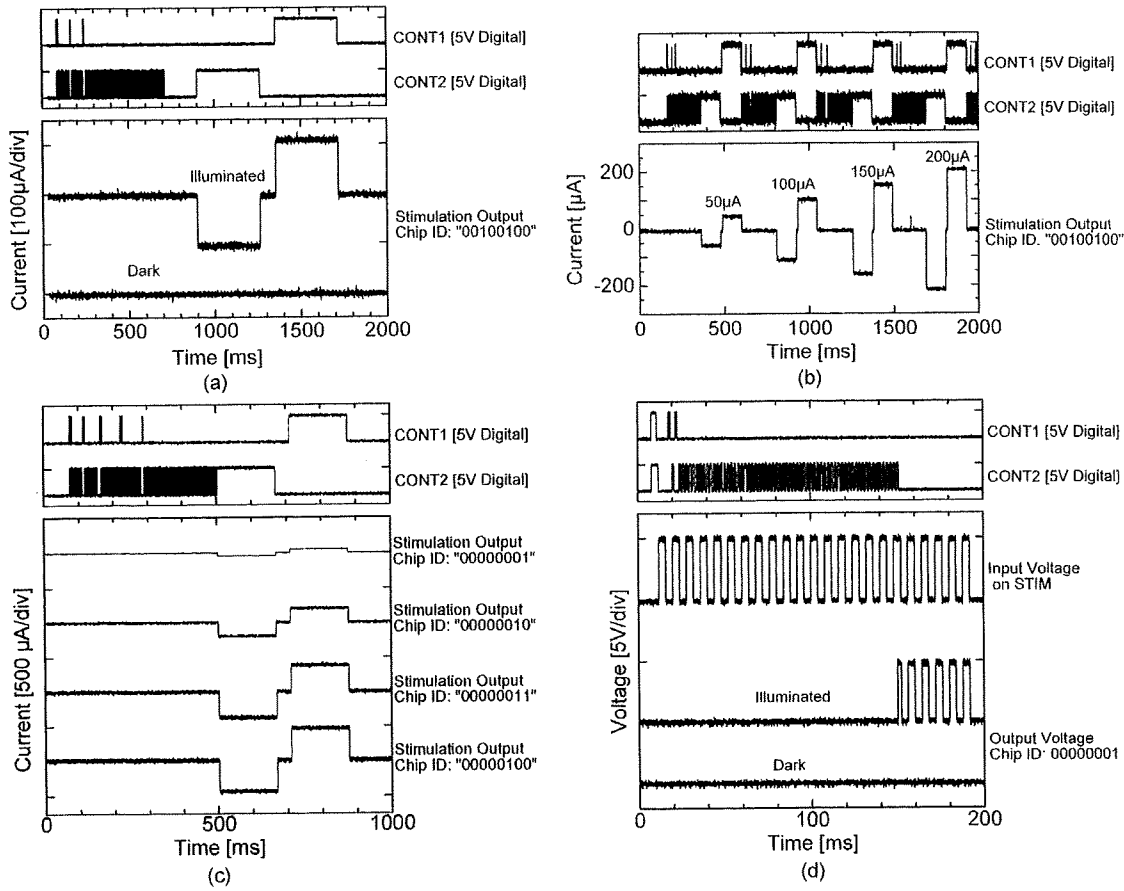

Fig. 5. Control and injection traces observed during the operation of the unit chips. (a) Biphasic current injection from a single unit chip using the on-chip stimulator. (b) Biphasic current injection from a single unit chip sequentially performed with different currents using the on-chip stimulator. (c) Biphasic current injection from four unit chips with different currents using the on-chip stimulator. (d) Connection measurement with a controlled voltage pulsed in the single-site relaying stimulation mode.

substrate with bus wirings and separated by a deep reactive ion etching process for flexible packaging [15]–[18]. We are also developing another connection structure using preconnected wires between the unit chips. We are developing this type of packaging to realize an improved form factor and better packaging yield. The detailed structure and packaging process shall be reported elsewhere.

In the present work, we designed three kinds of CMOS chips for functional verification and performance characterization. Table III shows the variations for the stimulator chips. The table includes the following: (a) a 41-unit radial stimulator; (b) a four-unit linear stimulator (two types of connection structures); and (c) a four-unit stimulator with the same design as previous works and the light-controlled stimulation developed in this paper.

III. Functional Characterization of the Unit Chip

Fig. 5(a)–(d) shows the experimentally obtained results showing the functions of the unit chip. Fig. 5(a)–(c) shows the operations using the on-chip stimulator. Fig. 5(a) and (b) was recorded using the unit chips with a chip ID of "00100100." In Fig. 5(c), we show the functionality of the multichip stimulation; the unit chips with IDs of "00000001," "00000010," "00000011," and "00000100" were used. Each stimulation electrode was connected to a voltage source kept at 2.5 V via a resistance of 2 kΩ. We have confirmed that the control logic of the present unit chip works at least up to a clock frequency of 40 MHz.

Fig. 5(d) shows the results of the single-site relaying stimulation mode using an external stimulator. Five-volt digital pulses are continuously applied on the STIM input of the unit chip, and the voltage of the stimulation electrode for the unit chip "00000001" was monitored.

The output traces are plotted in terms of current for operations using an on-chip stimulator [Fig. 5(a)–(c)] and in voltage for the single-site relaying stimulation mode [Fig. 5(d)].

In the demonstrations shown in Fig. 5(a)–(d), we can see the control sequences in the traces of CONT1 and CONT2. The control sequences consist of the value representing the number of pulses on CONT2 delimited by one or two pulses on CONT1. The sequences consist of the following:

1) reset with CONT1 = CONT2 = H;
2) input the address for the target unit chip (number of CONT2 pulses = target chip ID);
3) set the function and conditions for the stimulation (number of CONT2 pulses = command);
4) repeat steps 2) and 3) for all the unit chips to be used;

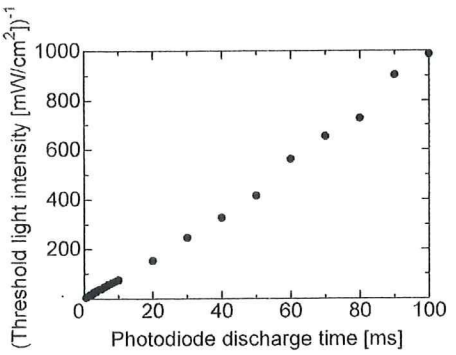

Fig. 6. Threshold light intensity as a function of the accumulation time for the light-controlled decision circuitry.

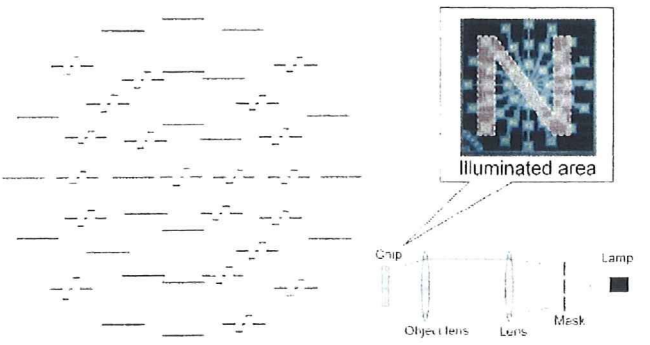

Fig. 7. Results of the image-based patterned current injection.

5) 256 pulses on CONT2 to transition the mode from control to stimulation;
6) stimulation with pulses on CONT1 and CONT2;
7) reset and restart for another stimulation procedure.

The mode transition from setting to stimulation is observed in Fig. 5(a)–(c). As described in the previous section, once the address is counted up to 256 and the ninth bit becomes H, the operation mode turns into the stimulation mode. In the stimulation mode, the current injection is triggered by CONT1 and CONT2. Positive injection is enabled by CONT1, and negative injection is enabled by CONT2, as shown in the figures.

In Fig. 5(a), we perform the minimum operation with single-site stimulation using the on-chip stimulator with the unit chip "00100100." We can see a single set of the addressing and commanding sequence on the CONT1 and CONT2 traces, followed by a single set of biphasic current injections controlled by CONT1 and CONT2.

In Fig. 5(b), we sequentially performed biphasic current injections with different conditions from the unit chip "00100100." The figure shows that the unit chip was correctly reset by the sequence CONT1 = CONT2 = H. We can change the condition even for each injection in the manner shown in Fig. 5(b).

In Fig. 5(c), we assigned different stimulation currents for four unit chips. We repeated steps 2) and 3) before we changed the operation mode. We successfully obtained the injection currents with the preset conditions.

Fig. 5(d) shows the demonstration result for the relaying stimulation operation. Just after the command to turn the selected unit chip (address = "00000001") into the relaying mode, the digital pulses applied on the STIM line are observed at the stimulation electrode of the unit chip "00000001."

In Fig. 5(a) and (d), we can see the output traces showing the light-controlled decision. The output signal was observed when the unit chip was illuminated. The results show that the light-controlled decision circuitry worked correctly. Fig. 6 shows the threshold light intensity as a function of the length of the last pulse for commanding. The threshold light intensity is in a reciprocal relationship with the photodiode discharge time. This result is consistent with the nature of the active pixel sensor circuitry and shows that the sensitivity (threshold light intensity) is widely adjustable. The discharge time by the dark current was typically 30 s for the present device.

IV. Image-Based Patterned Current Injection Using a Radially Aligned Retinal Stimulator

In order to verify the functionality of the image-based patterned stimulation, we performed an experimental demonstration in a "dry" situation. We used the radially aligned stimulator shown as chip (a) in Table III for the demonstration. The experiments in this section were performed with a die mounted on an 84-pin pin grid array package. We projected light patterns on the stimulator and set the function for all the unit chip cores as light-controlled stimulation with current amplitudes of 100 μA. After sending 41 sets of addressing and commanding pulses, we changed the operation mode into a stimulation mode. We then applied alternative pulses on CONT1 and CONT2 to generate the stimulation current pulses. We recorded the current profiles observed from the stimulation electrodes.

Fig. 7 shows the results of the experimentally performed image-based patterned current injection. The traces show the current profile recorded at the stimulation electrodes. The traces are placed to show the positions of the corresponding electrodes. As shown in Fig. 7, the organized unit chips work as a retinal stimulator with a functionality of image-based multisite stimulation.

V. *In Vivo* Demonstration of the Light-Controlled Stimulation on a Rabbit's Retina

We performed an *in vivo* experimental demonstration of the light-controlled retinal stimulation. We implemented the circuitry for light-controlled decisions (Fig. 3) on the previously developed multichip flexible retinal stimulator [15]–[18]. It is reasonable to use the previously developed platform and experimental protocol to demonstrate the functionality of the light-controlled stimulation.

In the present work, we used the same device packaging and experimental procedure as our previous report [18] except that we illuminated the stimulator with infrared (IR) light through the rabbit's retina. Since the rabbit (a Dutch black belted rabbit) was a wild type and its retina had not been degenerated, the wavelength chosen for the control light must be insensible by the rabbit's retina. We prepared an LED light source with a peak wavelength of 950 nm. A 3 × 3 array of IR LED (OSRAM, LD271H) was placed in front of the rabbit's eye. The distance between the implanted stimulator chip and the LED light source

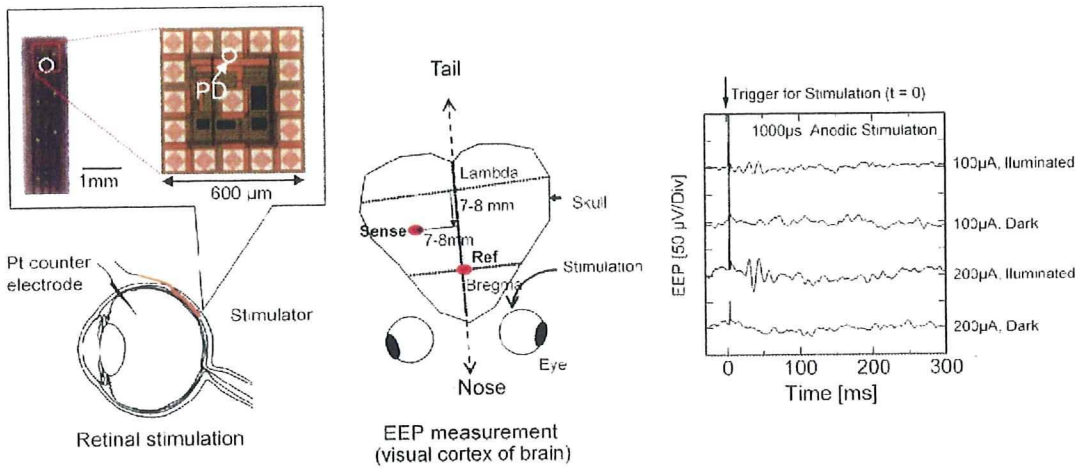

Fig. 8. Experimental setup and EEP traces observed in the *in vivo* retinal stimulation experiment using a rabbit.

was approximately 50 mm. We confirmed that no visually evoked potential (VEP) was observed by the IR illumination on the rabbit's retina.

After the surgical operation to implant the stimulator [18], we confirmed that a clear VEP response in the visual cortex of the animal's brain was observed when we used visible light. We can confirm that the rabbit was appropriately anesthetized and that the visual nerve system was ready for experiments.

In the *in vivo* experimental demonstration, we stimulated the rabbit's retina with an anodic constant-current injection. The pulse height was chosen to be between 50 and 300 μA, and the pulse duration was 1000 μs. The stimulation was performed 100 times with an interval of 2 s, and the signal on the visual cortex of the brain was averaged and recorded.

Fig. 8 shows the experimental setup [18] and results of the demonstration. The positions of the stimulator and the electrodes on the visual cortex are shown in Fig. 8. During the acute experiment, the stimulator was fixed at the insertion slit of the scleral pocket with a surgical suture. The inserted part of the stimulator was as flexible as it can fit the curvature, only with the pressure in the scleral pocket. The EEP traces show that the stimulation was successfully controlled by the IR light and caused differences in the response in the visual cortex of the rabbit's brain. For both conditions of 100 and 200 μA, clear responses were observed at 20–60 ms after the stimulation. The duration and waveform observed on the EEP traces suggest that the stimulation on the retina was enabled by only the illumination. Therefore, we can conclude that the rabbit's perception was controlled by light which was insensible to the rabbit's retina. This is a quite simple but direct demonstration of the concept for light-controlled (and image-based) retinal prosthesis. Since the spatial resolutions in both the retinal stimulation and EEP measurement on the visual cortex were limited in this paper, we cannot conclude that the sensation evoked by the current stimulator is a phosphene with a limited area. As future work, we need to perform more detailed animal experiments to confirm the functionality of evoking localized phosphenes that were observed in human experiments [14]. Biological effects in a long-term implantation are another important issue to be clarified.

VI. Conclusion

We have developed a CMOS LSI stimulator chip with the concept of a multichip architecture. The CMOS LSI stimulator system has the following features; 1) multisite stimulation using an on-chip stimulator; 2) light-controlled (imaging-based) stimulation; and 3) potential compatibility for spherical packaging. We can set different conditions for each unit chip connected to a single set of five-channel bus wiring and perform multisite constant-current biphasic retinal stimulation. We implemented a simple binary light-sensing circuitry on the unit chip to realize the image-based patterned stimulation on the retina.

We verified that all the implemented functionalities correctly work and characterize the performance of the circuitry. The demonstration for the image-based patterned current injection using radially aligned unit chips was performed in dry experiments. We also experimentally demonstrated the *in vivo* retinal stimulation based upon light-controlled decisions using light intensity measured at the stimulation site. It was a simplified demonstration for the concept of retinal prosthesis with on-site imaging.

References

[1] W. Liu and M. S. Humayun, "Retinal prosthesis," in *Proc. IEEE Int. Conf. Solid-State Circuits Dig. Tech. Papers*, Feb. 2004, pp. 218–219.

[2] L. Theogarajan, J. Wyatt, J. Rizzo, B. Drohan, M. Markova, S. Kelly, G. Swider, M. Raj, D. Shire, M. Gingerich, J. Lowenstein, and B. Yomtov, "Minimally invasive retinal prosthesis," in *Proc. IEEE Int. Conf. Solid-State Circuits Dig. Tech. Papers*, Feb. 2006, pp. 99–108.

[3] G. J. Suaning and N. H. Lovell, "CMOS neurostimulation ASIC with 100 channels, scaleable output, and bidirectional radio-frequency telemetry," *IEEE Trans. Biomed. Eng.*, vol. 48, no. 2, pp. 248–260, Feb. 2001.

[4] M. Ortmanns, N. Unger, A. Rocke, M. Gehrke, and H. J. Tietdke, "A 0.1 mm^2, digitally programmable nerve stimulation pad cell with high-voltage capability for a retinal implant," in *Proc. IEEE Int. Conf. Solid-State Circuits Dig. Tech. Papers*, Feb. 2006, pp. 89–98.

[5] A. Rothermel, V. Wieczorek, L. Liu, A. Stett, M. Gerhardt, A. Harscher, and S. Kibbel, "A 1600-pixel subretinal chip with DC-free terminals and ±2 V supply optimized for long lifetime and high stimulation efficiency," in *Proc. IEEE Int. Conf. Solid-State Circuits Dig. Tech. Papers*, Feb. 2008, pp. 144–146.

[6] J. D. Loudin, D. M. Simanovskii, K. Vijayraghavan, C. K. Sramek, A. F. Butterwick, P. Huie, G. Y. McLean, and D. V. Palanker, "Optoelectronic retinal prosthesis: System design and performance," *J. Neural Eng.*, vol. 4, no. 1, pp. S72–S84, Mar. 2007.

[7] A. Butterwick, A. Vankov, P. Huie, Y. Freyvert, and D. Palanker, "Tissue damage by pulsed electrical stimulation," *IEEE Trans. Biomed. Eng.*, vol. 54, no. 12, pp. 2261–2267, Dec. 2007.
[8] T. Tanaka, K. Sato, K. Komiya, T. Kobayashi, T. Watanabe, T. Fukushima, H. Tomita, H. Kurino, M. Tamai, and M. Koyanagi, "Fully implantable retinal prosthesis chip with photodetector and stimulus current generator," in *IEDM Tech. Dig.*, 2007, pp. 1015–1018.
[9] A. Y. Chow and V. Y. Chow, "Subretinal electrical stimulation of the rabbit retina," *Neurosci. Lett.*, vol. 225, no. 1, pp. 13–16, Mar. 1997.
[10] A. Y. Chow, V. Y. Chow, K. H. Packo, J. S. Pollack, G. A. Peyman, and R. Schuchard, "The artificial silicon retina microchip for the treatment of vision loss from retinitis pigmentosa," *Arch. Ophthalmol.*, vol. 122, no. 4, pp. 460–469, Apr. 2004.
[11] E. Zrenner, D. Besch, K. U. B. Schmidt, F. Gekeler, V. P. Gabel, C. Kuttenkeuler, H. Sachs, H. Sailer, B. Wilhelm, and R. Wilke, "Subretinal chronic multi-electrode arrays implanted in blind patients," in *Proc. Shanghai Int. Conf. Physiol. Biophys.*, 2006, p. 147.
[12] F. Gekeler, P. Szurman, S. Grisanti, U. Weiler, R. Claus, T.-O. Greiner, M. Volker, K. Kohler, E. Zrenner, and K. U. Bartz-Schmidt, "Compound subretinal prostheses with extra-ocular parts designed for human trials: Successful long-term implantation in pigs," *Graefe's Arch. Clin. Exp. Ophthalmol.*, vol. 245, no. 2, pp. 230–241, Feb. 2007.
[13] K. Nakauchi, T. Fujikado, H. Kanda, T. Morimoto, J. S. Choi, Y. Ikuno, H. Sakaguchi, M. Kamei, M. Ohji, T. Yagi, S. Nishimura, H. Sawai, Y. Fukuda, and Y. Tano, "Transretinal electrical stimulation by an intrascleral multichannel electrode array in rabbit eyes," *Graefe's Arch. Clin. Exp. Ophthalmol.*, vol. 243, no. 2, pp. 169–174, Feb. 2005.
[14] M. Kamei, T. Fujikado, H. Kanda, T. Morimoto, K. Nakauchi, H. Sakaguchi, Y. Ikuno, M. Ozawa, S. Kusaka, and Y. Tano, "Suprachoroidal transretinal stimulation (STS) artificial vision system for patients with retinitis pigmentosa," *Invest. Ophthalmol. Vis. Sci.*, vol. 47, p. 1537, 2006, E-Abstract.
[15] T. Tokuda, Y.-L. Pan, A. Uehara, K. Kagawa, M. Nunoshita, and J. Ohta, "Flexible and extendible neural interface device based on cooperative multi-chip CMOS LSI architecture," *Sens. Actuators A, Phys.*, vol. 122, no. 1, pp. 88–98, Jul. 2005.
[16] J. Ohta, T. Tokuda, K. Kagawa, T. Furumiya, A. Uehara, Y. Terasawa, M. Ozawa, T. Fujikado, and Y. Tano, "Silicon LSI-based smart stimulators for retinal prosthesis," *IEEE Eng. Med. Biol. Mag.*, vol. 25, no. 5, pp. 47–59, Sep./Oct. 2006.
[17] J. Ohta, T. Tokuda, K. Kagawa, S. Sugitani, M. Taniyama, A. Uehara, Y. Terasawa, K. Nakauchi, T. Fujikado, and Y. Tano, "Laboratory investigation of microelectronics-based stimulators for large-scale suprachoroidal transretinal stimulation (STS)," *J. Neural Eng.*, vol. 4, no. 1, pp. S85–S91, Mar. 2007.
[18] T. Tokuda, R. Asano, S. Sugitani, M. Taniyama, Y. Terasawa, M. Nunoshita, K. Nakauchi, T. Fujikado, Y. Tano, and J. Ohta, "Retinal stimulation on rabbit using CMOS-based multi-chip flexible stimulator toward retinal prosthesis," *Jpn. J. Appl. Phys.*, vol. 47, no. 4, pp. 3220–3225, 2008.
[19] M. Mahadevappa, J. D. Weiland, D. Yanai, I. Fine, R. Greenberg, and M. S. Humayun, "Perceptual thresholds and electrode impedance in three retinal prosthesis subjects," *IEEE Trans. Neural Syst. Rehabil. Eng.*, vol. 13, no. 2, pp. 201–206, Jun. 2005.
[20] J. W. Morley, Y. T. Wong, L. E. Hallum, S. C. Chen, N. Dommel, S. L. Cloherty, G. J. Suaning, and N. H. Lovell, "Optical imaging of electrically evoked visual signals in cats: I. Responses to corneal and intravitreal electrical stimulation," in *Proc. 29th Annu. Int. Conf. IEEE Eng. Med. Biol. Soc.*, Aug. 2007, pp. 1635–1638.

Takashi Tokuda (M'08) received the B.E. and M.E. degrees in electronic engineering and the Dr.Eng. degree in materials engineering from Kyoto University, Kyoto, Japan, in 1993, 1995, and 1998, respectively.

He has been an Assistant Professor since 1999 and has been an Associate Professor since 2008 with the Graduate School of Materials Science, Nara Institute of Science and Technology, Nara, Japan. His research interests include CMOS image sensors, bioimaging, and biosensors.

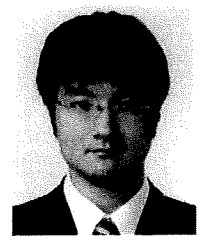

Kohei Hiyama received the B.E. degree from Osaka Kyoiku University, Osaka, Japan, in 2007 and the M.E. degree from Nara Institute of Science and Technology, Nara, Japan, in 2009.

He is currently with the Corporate Manufacturing Engineering Center, Toshiba Corporation, Yokohama, Japan.

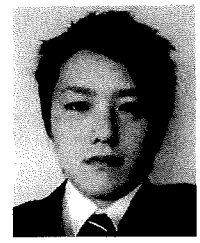

Shigeki Sawamura received the B.E. degree from Ryukoku University, Kyoto, Japan, in 2007 and the M.E. degree from Nara Institute of Science and Technology, Nara, Japan, in 2009.

He is currently with Canon Inc., Tokyo, Japan.

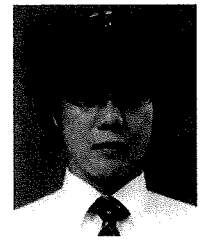

Kiyotaka Sasagawa (M'08) received the B.S. degree from Kyoto University, Kyoto, Japan, in 1999 and the M.E. and Ph.D. degrees in materials science from Nara Institute of Science and Technology, Nara, Japan, in 2001 and 2004, respectively.

From 2004 to 2008, he was a Researcher with the National Institute of Information and Communications Technology, Tokyo, Japan. In 2008, he joined Nara Institute of Science and Technology, where he is currently an Assistant Professor. His research interests involve bioimaging, biosensing, and electromagnetic field measurement.

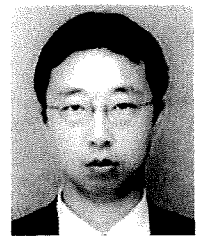

Yasuo Terasawa received the B.E. and M.E. degrees from Tohoku University, Sendai, Japan, in 1996 and 1998, respectively, and the Ph.D. degree from Nara Institute of Science and Technology, Nara, Japan, in 2009.

He is currently with the Vision Institute, R&D Division, NIDEK Company, Ltd., Gamagori, Japan.

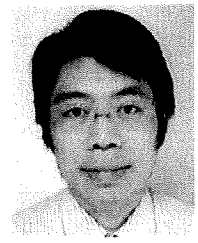

Kentaro Nishida received the M.D. degree from Osaka University, Osaka, Japan, where he is currently working toward the Ph.D. degree.

Yoshiyuki Kitaguchi received the M.D. degree from Osaka University, Osaka, Japan, where he is currently working toward the Ph.D. degree.

His research interests include evaluating retinal damages with a retinal imaging device, i.e., adaptive optics fundus camera.

Takashi Fujikado received the B.E. and M.E. degrees from The University of Tokyo, Tokyo, Japan, and the M.D. and Ph.D. degrees from Osaka University, Osaka, Japan.

He is currently a Professor of applied visual science with the Graduate School of Medicine, Osaka University. He has been involved in the field of neuro-ophthalmology and ophthalmic optics.

Dr. Fujikado is a member of the Consortium of Artificial Retina in Japan, where he is working on the functional assessment of artificial retina.

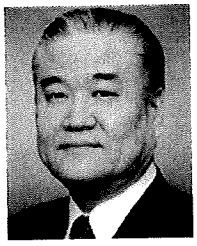

Yasuo Tano received the M.D. and Ph.D. degrees from Osaka University, Osaka, Japan.

He was with the Department of Ophthalmology, Graduate School of Medicine, Osaka University. He conducted the Retinal Prosthesis Project Team consisting of Osaka University, Nara Institute of Science and Technology, Nara, Japan, and Nidek Company, Ltd.

Dr. Tano was the former President of the Japanese Ophthalmological Society and was the current President of Asia Pacific Academy of Ophthalmology. He passed away on January 31, 2009.

Jun Ohta (M'97) received the B.E., M.E., and Dr.Eng. degrees in applied physics from The University of Tokyo, Tokyo, Japan, in 1981, 1983, and 1992, respectively.

In 1983, he joined Mitsubishi Electric Corporation, Hyogo, Japan, where he has been engaged in the research on optoelectronic integrated circuits, optical neural networks, and artificial retina chips. From 1992 to 1993, he was a Visiting Researcher with the Optoelectronics Computing Systems Center, University of Colorado, Boulder. Since 1998, he has been an Associate Professor with the Graduate School of Materials Science, Nara Institute of Science and Technology, Nara, Japan, where, since 2004, he has been a Professor. His current research interests include vision chips, complimentary metal–oxide–semiconductor image sensors, retinal prosthesis devices, biophotonic large-scale integrations, and integrated photonic devices.